

# Seismicity trends and detachment fault structure at 13°N, Mid-Atlantic Ridge

R. Parnell-Turner<sup>1</sup>, R.A. Sohn<sup>2</sup>, C. Peirce<sup>3</sup>, T.J. Reston<sup>4</sup>, C.J. MacLeod<sup>5</sup>, R.C. Searle<sup>3</sup> and N.M. Simão<sup>3</sup>

<sup>1</sup>Scripps Institution of Oceanography, University of California, San Diego, California 92037, USA

<sup>2</sup>Woods Hole Oceanographic Institution, Woods Hole, Massachusetts 02543, USA

<sup>3</sup>Department of Earth Sciences, Durham University, Durham DH1 3LE, UK

<sup>4</sup>School of Geography, Earth and Environmental Sciences, University of Birmingham, Birmingham B15 2TT, UK

<sup>5</sup>School of Earth and Ocean Sciences, Cardiff University, Cardiff CF10 3AT, UK

## ABSTRACT

At slow-spreading ridges, plate separation is commonly partly accommodated by slip on long-lived detachment faults, exposing upper mantle and lower crustal rocks on the seafloor. However, the mechanics of this process, the subsurface structure, and the interaction of these faults remain largely unknown. We report the results of a network of 56 ocean-bottom seismographs (OBSs), deployed in 2016 at the Mid-Atlantic Ridge near 13°N, that provided dense spatial coverage of two adjacent detachment faults and the intervening ridge axis. Although both detachments exhibited high levels of seismicity, they are separated by an ~8-km-wide aseismic zone, indicating that they are mechanically decoupled. A linear band of seismic activity, possibly indicating magmatism, crosscuts the 13°30'N domed detachment surface, confirming previous evidence for fault abandonment. Farther south, where the 2016 OBS network spatially overlapped with a similar survey done in 2014, significant changes in the patterns of seismicity between these surveys are observed. These changes suggest that oceanic detachments undergo previously unobserved cycles of stress accumulation and release as plate spreading is accommodated.

## INTRODUCTION

At spreading ridges with a low or variable magma supply, faulting is commonly heterogeneous, giving rise to a variety of deformation styles, including long-lived detachment faults (Cannat et al., 1995; Blackman et al., 1998; Escartín et al., 2003; Ildefonse et al., 2007; MacLeod et al., 2009). Recognition of this detachment mode of spreading is considered to be one of the most important recent advances in plate tectonics (Mutter and Karson, 1992; Cannat et al., 1995; Cann et al., 1997; Dick et al., 2003; Escartín and Canales, 2011; Reston and McDermott, 2011). We now know that detachment faults initiate at steep angles (~70°) at depths ≥10 km, rotate to low angles (~15°) in the shallower crust, and can slip for several million years (Cann et al., 1997; Dick et al., 2003; deMartin et al., 2007; Smith et al., 2008; Morris et al., 2009). These faults can bring lower crustal and upper mantle rocks to the surface in domes known as oceanic core complexes (OCCs) or generate gently undulating peridotite-dominated

expanses of seafloor (Cannat et al., 2006; Sauter et al., 2013; Reston, 2018).

Here we present the results of a local earthquake survey conducted in 2016 at the 13°N segment of the Mid-Atlantic Ridge that encompasses two detachments at different stages of the faulting life cycle. The observed seismicity patterns provide new insight into the mechanical evolution of OCCs and their along-axis structure. Our 2016 experiment is located in the area of a similar survey undertaken in 2014. The combined results of the two surveys allow us to assess temporal variations in detachment fault seismicity for the first time.

## APPROACH

We conducted repeat micro-earthquake surveys over and between the 13°20'N and 13°30'N OCCs at the Mid-Atlantic Ridge, chosen because these OCCs have been extensively mapped, imaged, and sampled over the past decade (Smith et al., 2008; MacLeod et al., 2009; Mallows and Searle, 2012; Craig and Parnell-Turner, 2017;

Escartín et al., 2017; Parnell-Turner et al., 2017; Peirce et al., 2019, 2020; Searle et al., 2019; Simão et al., 2020). The presence of two closely spaced OCCs led to the conflicting hypotheses that they might represent either the exposed part of a single, more extensive undulating detachment (e.g., Smith et al., 2008), or two mechanically distinct, locally controlled structures (Smith et al., 2008; MacLeod et al., 2009). The first micro-earthquake survey was an approximately 6 month experiment from April to October 2014, with 25 short-period ocean-bottom seismographs (OBSs) deployed along ~10 km of the ridge axis, which yielded new insight into the internal deformation of the fault footwall (Parnell-Turner et al., 2017). The second survey, conducted 15 months later in early 2016, was a shorter, ~11 day, experiment employing a network of 56 OBSs distributed along ~30 km of the ridge axis, including both the 13°20'N and 13°30'N OCCs. Stations were arranged in a grid with 2–5 km inter-element spacing and an aperture covering the domes and footwalls of both OCCs and the adjacent neovolcanic zone (Fig. 1A). Although the duration was shorter (limited by the gaps in an active-source survey shot into the OBSs), the high seismicity rate (23 events per day per kilometer of ridge axis; Parnell-Turner et al., 2017) and larger footprint of the second survey allowed the identification of primary fault structures associated with the two OCCs and the intervening portion of the ridge axis.

## RESULTS

During the 2016 experiment, we detected 21,332 events on four or more OBSs using a standard triggering algorithm, giving an event rate of >82 per hour. Of these events, 5511 could

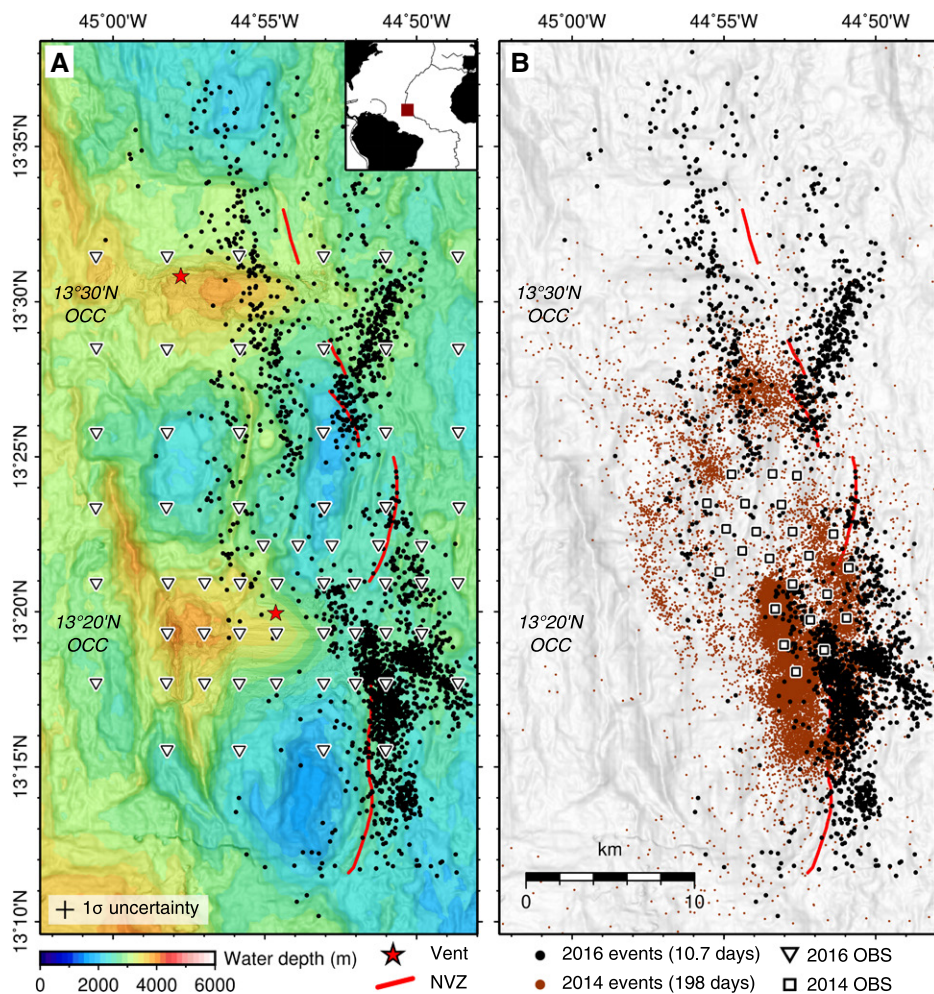


**Figure 1. Bathymetry (Searle et al., 2019) and seismicity near 13°20'N, Mid-Atlantic Ridge. (A) Inset shows study site (red box) and plate boundaries (black lines). Black dots are relocated micro-earthquakes recorded by ocean-bottom seismographs (OBSs) (triangles) over ~11 days in 2016; red line is neovolcanic zone (NVZ; Parnell-Turner et al., 2017); red stars are hydrothermal vents. Locations of oceanic core complexes (OCCs) are shown by 13°20'N and 13°30'N labels; cross size is average 68% confidence level in horizontal location uncertainty (0.9 km). (B) Same area as A, with brown dots indicating micro-earthquakes recorded over 198 days in 2014 (squares are OBSs; Parnell-Turner et al., 2017).**

be reliably located using *P*- and *S*-wave arrival times and a velocity model derived from the active-source experiment (Baillard et al., 2014; Peirce et al., 2019; Simão et al., 2020). The methods used here, including the velocity model, are the same as those used for the 2014 experiment (Parnell-Turner et al., 2017). Relative relocation methods were used to refine hypocenter estimates (see the Supplemental Material<sup>1</sup> for methods), yielding a final catalog of 2405 events (Figs. 1 and 2). First-motion focal mechanisms (Fig. 3) were estimated for events located within the network aperture with hypocentral misfit of <250 ms (Hardebeck and Shearer, 2002).

<sup>1</sup>Supplemental Material. Additional information and figures describing the acquisition and processing of the micro-earthquake data set, including links to data repository and 3-D visualization of the earthquake catalog. Please visit <https://doi.org/10.1130/GEOL.S.13082285> to access the supplemental material, and contact [editing@geosociety.org](mailto:editing@geosociety.org) with any questions.

Seismic moment and local magnitudes were estimated using displacement spectra (2–40 Hz) recorded by the vertical OBS channel, yielding a magnitude of completeness,  $M_{LC} = 0.7$  (Fig. S1 in the Supplemental Material).

The 13°30'N and 13°20'N OCCs have high levels of micro-earthquake activity. Both generate a distinct band of relatively deep (~6–12 km below seafloor [bsf]) seismicity ~4 km east of the OCC domes, and the overall north-northwest trend of the microseismicity corresponds to the broader trend of the axial valley and local axial volcanic ridges (Fig. 1A). This deep band of seismicity was also observed at the 13°20'N OCC during the 2014 survey (the band east of the 13°30'N OCC could not be resolved by the 2014 survey), and these events are interpreted to represent slip on the detachment surface, likely extending into the fault root zone (Parnell-Turner et al., 2017; Fig. 2). This band of seismicity deepens from 5 to 10 km bsf over a distance

of ~6 km heading south from the 13°20'N detachment (Fig. 2D), suggesting the fault surface deepens where it encounters thicker or cooler lithosphere. This interpretation is tentative due to reduced hypocentral resolution in this region, which is beyond the network aperture. High levels of persistent seismicity along the basal portion of the detachment surface have also been observed at the Trans-Atlantic Geotraverse (TAG) detachment on the Mid-Atlantic Ridge at 26°N (deMartin et al., 2007), suggesting that this type of activity may be common to active oceanic detachment faults.

Between the 13°30'N and 13°20'N OCCs, there is an ~8 km zone (from 13°22'N to 13°25'N) that was effectively aseismic during both the 2014 and 2016 surveys (Fig. 1). This aseismic zone is much longer than the lateral uncertainties in the hypocenter estimates, and it is located near the center of the 2016 OBS network, where detectability bias is negligible. We thus find that the 13°30'N and 13°20'N OCCs are separated by an ~8 km length of ridge axis that did not experience significant seismic deformation during either observation interval.

The 2016 micro-earthquake survey imaged a linear band of micro-earthquakes that cuts the 13°30'N OCC dome on a trend of ~355° and at a depth of ~6–7 km bsf. Focal mechanism estimates are not available for this band of micro-earthquakes due to network geometry, but remotely operated vehicle (ROV) surveys of the 13°30'N dome surface have shown that it is disrupted by normal faulting, fissuring, and mass wasting (Escartín et al., 2017). These observations suggest that the 13°30'N OCC is being dissected by a new fault surface. The band of seismicity extends to a set of linear volcanic ridges and a seamount south of the dome that are known to have been recently magmatically active (Mallows and Searle, 2012; Escartín et al., 2017; Searle et al., 2019) and that generated a swarm of 276 events over ~3 days during the 2014 survey. The new fault surface dissecting the OCC may, therefore, be associated with magmatic processes, including possibly lateral dike propagation either into or out of the OCC interior (Mallows and Searle, 2012).

Marked differences between the seismicity patterns observed during the 2014 and 2016 surveys are evident, even considering the different instrument spacing, aperture, and duration of the two studies. The intense band of intermediate-depth (3.5–6.5 km) compressional seismicity observed east of the 13°20'N detachment throughout the 2014 survey is completely absent in the 2016 records (see Fig. 2B). This stark change in the nature of footwall deformation suggests that compressive bending stresses may be released episodically, rather than continuously, during footwall exhumation, even though slip on the deeper parts of the fault surface appears to be continuous. Whereas micro-earthquake

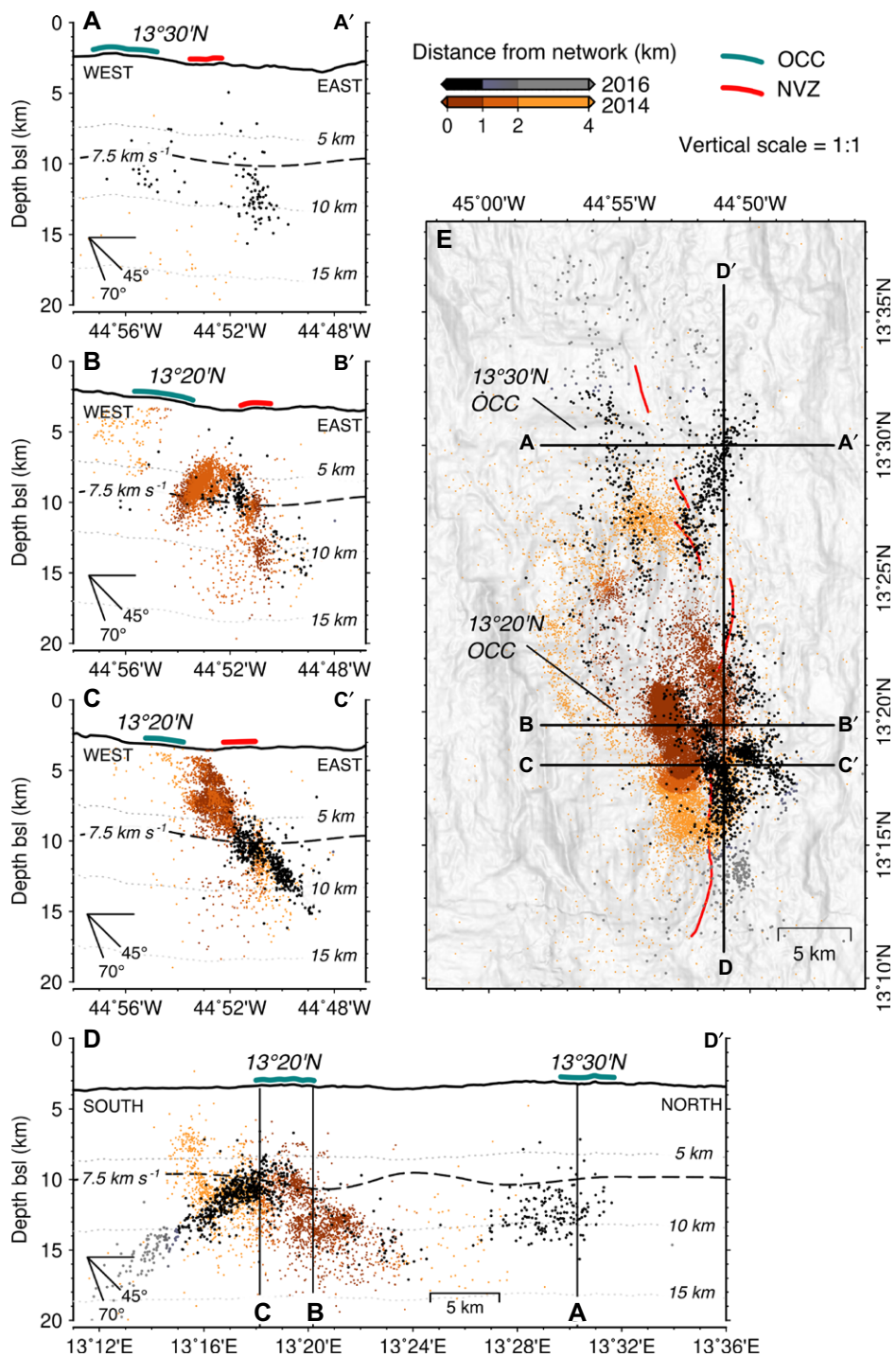


**Figure 2.** Depth profiles with seismicity. (A–D) Cross sections showing bathymetry (black lines) and micro-earthquakes located within 2 km of profile from 2014 and 2016 experiments (dots; see key); teal lines mark detachment fault scarps; red lines are the projected location of the neovolcanic zone (NVZ) (Parnell-Turner et al. 2017); labeled dashed gray lines show depths below seafloor (bsf); dashed black lines are  $7.5 \text{ km s}^{-1}$  velocity contour, from Simao et al. [2020]). (E) Profile locations marked as labeled black lines. OCC—oceanic core complex.

focal mechanisms exhibit a distinct spatial pattern in the 2014 survey, with compressive mechanisms in the footwall and extensional mechanisms on the putative fault surface, the limited focal mechanisms available from the 2016 survey exhibit a much more random pattern, without any appreciable spatial correlations. Although the 2014 and 2016 surveys used

networks with different apertures and spacings, the focal mechanism differences remain striking and suggest that the bending stresses released in 2014 may have modified the local stress field.

## DISCUSSION

Our results provide new insight into the subsurface fault structures associated with the

formation, maintenance, and abandonment of OCCs and indicate that detachments undergo previously unobserved short-term deformation cycles.

## Subsurface Fault Structure and Linkages

We observed a seismic gap between the two oceanic detachments in both the 2014 and 2016 deployments. Both surveys also detected activity on each detachment fault, and while the nature of this activity varied, the aseismic character of the region between them remained unchanged. Hence it is unlikely that the  $13^{\circ}20'N$  and  $13^{\circ}30'N$  OCCs are linked by a single fault surface, and instead are mechanically decoupled by an  $\sim 8\text{-km}$ -long aseismic zone (Fig. 4). This observation supports evidence from seismic velocity and crustal magnetization studies that the two OCCs are structurally distinct features and not part of a single, undulating fault surface (Peirce et al., 2019, 2020; Searle et al., 2019). The apparent seismic gap could be explained by an along-axis transition from brittle detachment faulting to ductile shear zone deformation, as suggested at other detachments (e.g., Hansen et al., 2013). This interpretation is consistent with mechanical decoupling of the detachments because strain would not be transmitted across the ductile zone.

The  $13^{\circ}30'N$  and  $13^{\circ}20'N$  OCCs seem to be at different stages of evolution. Seismicity at the  $13^{\circ}20'N$  OCC is consistent with ongoing detachment faulting and continued development of the OCC. At the  $13^{\circ}30'N$  OCC, however, the OCC dome is crosscut by a distinct band of events that links to a magmatically active region to the south. Seismic dissection of the OCC dome is consistent with sidescan sonar, video imagery, and active-source seismic data indicating that the  $13^{\circ}30'N$  detachment is gradually being pulled apart and abandoned (MacLeod et al., 2009; Mallows and Searle, 2012; Parnell-Turner et al., 2018b; Peirce et al., 2019, 2020). The linkage of the crosscutting seismicity to an active volcanic feature just south of the OCC dome, along with the presence of a high-temperature vent field (Semenov) on the dome itself (Cherkashov et al., 2008; Pertsev et al., 2012; Escartín et al., 2017), suggests that the structural realignment may be associated with an influx of magma. However, no seismic low-velocity zones have been detected in this region (Peirce et al., 2019, 2020).

## Temporal Variability

The  $13^{\circ}20'N$  and  $13^{\circ}30'N$  OCCs both generated continuously high levels of seismicity on what we interpret to be the lower portion of the main detachment fault surface. In contrast, we did not detect seismicity on the shallow, gently dipping portion of the main fault surfaces at either OCC in the 2014 or 2016 surveys. This same dichotomy between the seismic behaviors

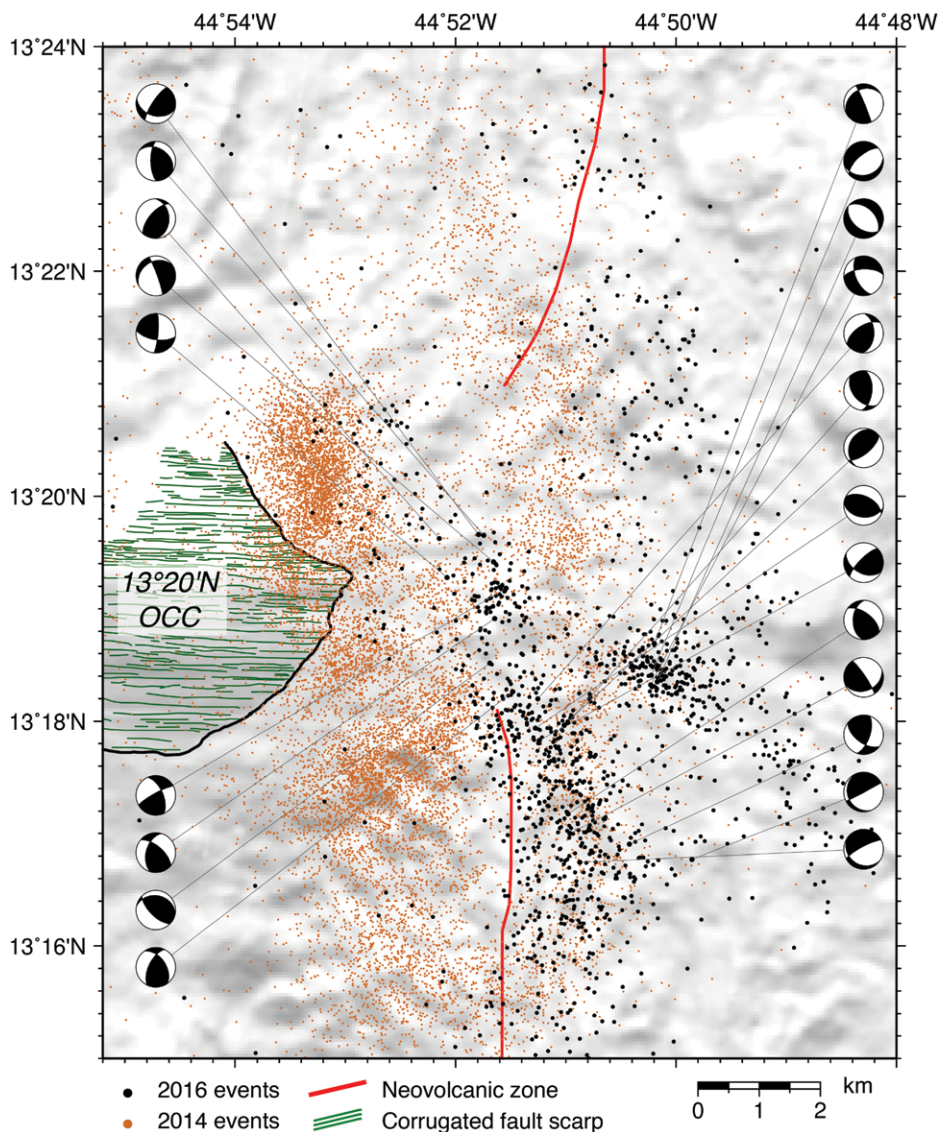


**Figure 3. Focal mechanisms.** Map is centered east of the 13°20'N oceanic core complex (OCC), showing events from 2014 and 2016 experiments (orange and blue colored dots, respectively), selected first-motion focal mechanisms from 2016 (lower-hemisphere projection), neovolcanic zone (Parnell-Turner et al., 2017), and fault scarp corrugations (Parnell-Turner et al., 2018a).

of the upper versus lower crust is seen elsewhere at slow- and ultraslow-spreading ridges, such as at the TAG detachment on the Mid-Atlantic Ridge (deMartin et al., 2007) and on detachments at the Southwest Indian Ridge (Yu et al., 2018). Although OCCs at 13°N, TAG, and the Southwest Indian Ridge are at different stages of the detachment faulting life cycle, they all exhibit this same difference in seismicity on the upper versus lower portion of the fault, suggesting it could be a common characteristic of active oceanic detachments. Although shallow seismicity on the detachment faults was not observed during either of our surveys, this region has generated three large ( $M_w$  5.5–5.7) earthquakes since 2008 (Craig and Parnell-Turner, 2017). Waveform modeling indicates these were likely normal-faulting events with centroid depths of 5–6 km bsf with ruptures that propagated to

within <2 km of the surface (Craig and Parnell-Turner, 2017). Brittle behavior is consistent with quartz cementation found in the shallow portion of the 13°20'N OCC, which favors deformation over stable sliding or ductile creep (Bonnemains et al., 2017). This combined evidence suggests that shallow portions of the fault system deform via large, infrequent events rather than high levels of low-magnitude seismicity (Fig. 4).

The strikingly different patterns of seismic activity and focal mechanisms observed during the 2014 and 2016 surveys of the 13°20'N OCC demonstrate that the rate and style of deformation associated with detachment faults varies on time scales as short as 15 months. Compressional internal deformation of the footwall was recorded throughout the 6 months of recording in 2014 but is almost completely absent from the data recorded early in 2016. These observa-

tions suggest a complex mechanical coupling between the deep part of the detachment near the fault root zone, which appears to effectively slip continuously via ubiquitous low-magnitude events, and the shallow part where it rolls over to low angles, which appears to slip aseismically or via infrequent, large events (Craig and Parnell-Turner, 2017). We hypothesize that this mismatch results in a cyclical pattern of footwall internal stress, where bending stresses accumulate slowly over time and are released episodically via swarms of compressive events, as observed over at least 6 months in the 2014 survey.

Our results demonstrate that oceanic detachment faults undergo deformation cycles on multiple time scales. Detachments are created and abandoned due to subsurface structural changes on time scales of up to millions of years, likely associated with magmatic processes on regional length scales. On annual time scales, the contrast between continuous slip in the fault root zone versus episodic slip on the shallow portion of the fault may cause episodic compression in the footwall. Our results also show that along-axis neighboring detachment faults can be mechanically decoupled and behave as discrete, ephemeral systems.

#### ACKNOWLEDGMENTS

This work was funded by UK Natural Environmental Research Council (NERC) grants NE/J02029X/1, NE/J022551/1, and NE/J021741/1 and by U.S. National Science Foundation grants OCE-1458084 and OCE-1839727. OBSs were provided by NERC UK Ocean-Bottom Instrumentation Facility (Minshull et al., 2005). We thank all those involved with the data acquisition, and I. Grevemeyer and two anonymous reviewers for their helpful input.

#### REFERENCES CITED

- Baillard, C., Crawford, W.C., Ballu, V., Hibert, C., and Mangeny, A., 2014, An automatic kurtosis-based P- and S-phase picker designed for local seismic networks: *Bulletin of the Seismological Society of America*, v. 104, p. 394–409, <https://doi.org/10.1785/0120120347>.
- Blackman, D.K., Cann, J.R., Janssen, B., and Smith, D.K., 1998, Origin of extensional core complexes: Evidence from the Mid-Atlantic Ridge at Atlantis fracture zone: *Journal of Geophysical Research*, v. 103, p. 21,315–21,333, <https://doi.org/10.1029/98JB01756>.
- Bonnemains, D., Escartín, J., Mével, C., Andreani, M., and Verlaguet, A., 2017, Pervasive silicification and hanging wall overplating along the 13°20'N oceanic detachment fault (Mid-Atlantic Ridge): *Geochemistry Geophysics Geosystems*, v. 18, p. 2028–2053, <https://doi.org/10.1002/2017GC006846>.
- Cann, J.R., Blackman, D.K., Smith, D.K., McAllister, E., Janssen, B., Mello, S., Avgerinos, E., Pascoe, A.R., and Escartín, J., 1997, Corrugated slip surfaces formed at ridge-transform intersections on the Mid-Atlantic Ridge: *Nature*, v. 385, p. 329–332, <https://doi.org/10.1038/385329a0>.
- Cannat, M., et al., 1995, Thin crust, ultramafic exposures, and rugged faulting patterns at the Mid-Atlantic Ridge (22°–24°N): *Geology*, v. 23, p. 49–52, [https://doi.org/10.1130/0091-7613\(1995\)023<0049:TCUEAR>2.3.CO;2](https://doi.org/10.1130/0091-7613(1995)023<0049:TCUEAR>2.3.CO;2).

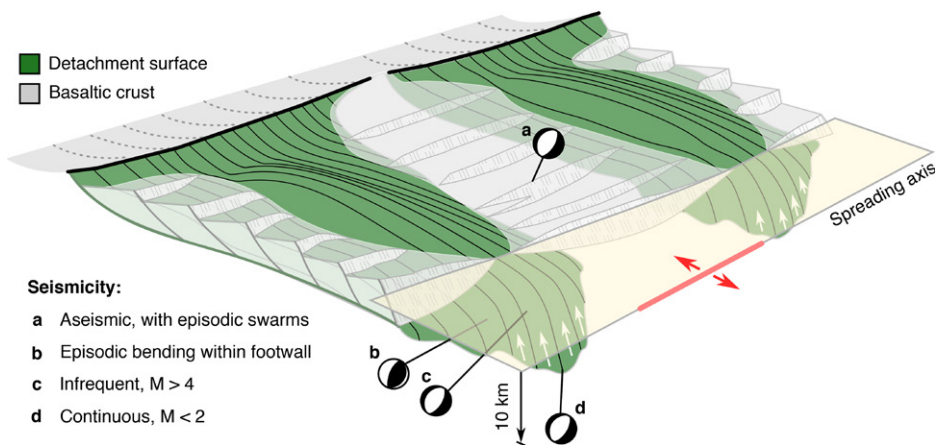


**Figure 4. Detachment fault mechanics.** Cartoon shows two neighboring detachment faults, mechanically decoupled along axis, with spatially variable deformation (labels a–d). Green polygons with black lines are the detachment footwall surface with plate-spreading parallel corrugations; white arrows show slip in the fault root zone; thick black lines are fault breakaways; gray shading is basaltic crust dissected by small-offset steep normal faults; yellow shading is the hanging-wall apron; red line and arrows show the magmatic portion of the spreading axis; zones of seismicity are marked a–d, with associated schematic lower-hemisphere focal mechanisms.

Cannat, M., Sauter, D., Mendel, V., Ruellan, E., Okino, K., Escartín, J., Comber, V., and Baala, M., 2006, Modes of seafloor generation at a melt-poor ultraslow-spreading ridge: *Geology*, v. 34, p. 605–608, <https://doi.org/10.1130/G22486.1>.

Cherkashov, G., Bel'tenev, V., Ivanov, V., Lazareva, L., Samovarov, M., Shilov, V., Stepanova, T., Glasby, G.P., and Kuznetsov, V., 2008, Two new hydrothermal fields at the Mid-Atlantic Ridge: *Marine Georesources and Geotechnology*, v. 26, p. 308–316, <https://doi.org/10.1080/10641190802400708>.

Craig, T.J., and Parnell-Turner, R., 2017, Depth-varying seismogenesis on an oceanic detachment fault at 13°20'N on the Mid-Atlantic Ridge: *Earth and Planetary Science Letters*, v. 479, p. 60–70, <https://doi.org/10.1016/j.epsl.2017.09.020>.

deMartin, B.J., Sohn, R.A., Canales, J.P., and Humphris, S.E., 2007, Kinematics and geometry of active detachment faulting beneath the Trans-Atlantic Geotraverse (TAG) hydrothermal field on the Mid-Atlantic Ridge: *Geology*, v. 35, p. 711–714, <https://doi.org/10.1130/G23718A.1>.

Dick, H.J.B., Lin, J., and Schouten, H., 2003, An ultraslow-spreading class of ocean ridge: *Nature*, v. 426, p. 405–412, <https://doi.org/10.1038/nature02128>.

Escartín, J., and Canales, J.P., 2011, Detachments in oceanic lithosphere: Deformation, magmatism, fluid flow, and ecosystems: *Eos (Transactions, American Geophysical Union)*, v. 92, p. 31, <https://doi.org/10.1029/2011EO040003>.

Escartín, J., Mével, C., MacLeod, C.J., and McCaig, A.M., 2003, Constraints on deformation conditions and the origin of oceanic detachments: The Mid-Atlantic Ridge core complex at 15°45'N: *Geochemistry Geophysics Geosystems*, v. 4, 1067, <https://doi.org/10.1029/2002GC000472>.

Escartín, J., et al., 2017, Tectonic structure, evolution, and the nature of oceanic core complexes and their detachment fault zones (13°20'N and 13°30'N, Mid Atlantic Ridge): *Geochemistry Geophysics Geosystems*, v. 18, p. 1451–1482, <https://doi.org/10.1002/2016GC006775>.

Hansen, L.N., Cheadle, M.J., John, B.E., Swapp, S.M., Dick, H.J.B., Tucholke, B.E., and Tivey, M.A.,

2013, Mylonitic deformation at the Kane oceanic core complex: Implications for the rheological behavior of oceanic detachment faults: *Geochemistry Geophysics Geosystems*, v. 14, p. 3085–3108, <https://doi.org/10.1002/ggge.20184>.

Hardebeck, J.L., and Shearer, P.M., 2002, A new method for determining first-motion focal mechanisms: *Bulletin of the Seismological Society of America*, v. 92, p. 2264–2276, <https://doi.org/10.1785/0120010200>.

Ildefonse, B., Blackman, D.K., John, B.E., Ohara, Y., Miller, D.J., and MacLeod, C.J., 2007, Oceanic core complexes and crustal accretion at slow-spreading ridges: *Geology*, v. 35, p. 623–626, <https://doi.org/10.1130/G23531A.1>.

MacLeod, C.J., Searle, R.C., Murton, B.J., Casey, J.F., Mallows, C., Unsworth, S.C., Achenbach, K.L., and Harris, M., 2009, Life cycle of oceanic core complexes: *Earth and Planetary Science Letters*, v. 287, p. 333–344, <https://doi.org/10.1016/j.epsl.2009.08.016>.

Mallows, C., and Searle, R.C., 2012, A geophysical study of oceanic core complexes and surrounding terrain, Mid-Atlantic Ridge 13°N–14°N: *Geochemistry Geophysics Geosystems*, v. 13, Q0AG08, <https://doi.org/10.1029/2012GC004075>.

Minshull, T.A., Sinha, M.C., and Peirce, C., 2005, Multi-disciplinary, sub-seabed geophysical imaging: *Sea Technology*, v. 46, p. 27–31.

Morris, A., Gee, J.S., Pressling, N., John, B.E., MacLeod, C.J., Grimes, C.B., and Searle, R.C., 2009, Footwall rotation in an oceanic core complex quantified using reoriented Integrated Ocean Drilling Program core samples: *Earth and Planetary Science Letters*, v. 287, p. 217–228, <https://doi.org/10.1016/j.epsl.2009.08.007>.

Mutter, J.C., and Karson, J.A., 1992, Structural processes at slow-spreading ridges: *Science*, v. 257, p. 627–634, <https://doi.org/10.1126/science.257.5070.627>.

Parnell-Turner, R., Sohn, R.A., Peirce, C., Reston, T.J., MacLeod, C.J., Searle, R.C., and Simão, N.M., 2017, Oceanic detachment faults generate compression in extension: *Geology*, v. 45, p. 923–926, <https://doi.org/10.1130/G39232.1>.

Parnell-Turner, R., Escartín, J., Olive, J.-A., Smith, D.K., and Petersen, S., 2018a, Genesis of corru-

gated fault surfaces by strain localization recorded at oceanic detachments: *Earth and Planetary Science Letters*, v. 498, p. 116–128, <https://doi.org/10.1016/j.epsl.2018.06.034>.

Parnell-Turner, R., Mittelstaedt, E., Kurz, M.D., Jones, M.R., Soule, S.A., Klein, F., Wanless, V.D., and Fornari, D.J., 2018b, The final stages of slip and volcanism on an oceanic detachment fault at 13°48'N, Mid-Atlantic Ridge: *Geochemistry Geophysics Geosystems*, v. 19, p. 3115–3127, <https://doi.org/10.1029/2018GC007536>.

Peirce, C., Reveley, G., Robinson, A.H., Funnell, M.J., Searle, R.C., Simão, N.M., MacLeod, C.J., and Reston, T.J., 2019, Constraints on crustal structure of adjacent OCCs and segment boundaries at 13°N on the Mid-Atlantic Ridge: *Geophysical Journal International*, v. 217, p. 988–1010, <https://doi.org/10.1093/gji/ggz074>.

Peirce, C., Robinson, A.H., Funnell, M.J., Searle, R.C., MacLeod, C.J., and Reston, T.J., 2020, Magmatism versus serpentinization—Crustal structure along the 13°N segment at the Mid-Atlantic Ridge: *Geophysical Journal International*, v. 221, p. 981–1001, <https://doi.org/10.1093/gji/ggaa052>.

Pertsev, A.N., Bortnikov, N.S., Vlasov, E.A., Beltenev, V.E., Dobretsova, I.G., and Ageeva, O.A., 2012, Recent massive sulfide deposits of the Semenov ore district, Mid-Atlantic Ridge, 13°31'N: Associated rocks of the oceanic core complex and their hydrothermal alteration: *Geology of Ore Deposits*, v. 54, p. 334–346, <https://doi.org/10.1134/S1075701512050030>.

Reston, T.J., 2018, Flipping detachments: The kinematics of ultraslow spreading ridges: *Earth and Planetary Science Letters*, v. 503, p. 144–157, <https://doi.org/10.1016/j.epsl.2018.09.032>.

Reston, T.J., and McDermott, K.G., 2011, Successive detachment faults and mantle unroofing at magma-poor rifted margins: *Geology*, v. 39, p. 1071–1074, <https://doi.org/10.1130/G32428.1>.

Sauter, D., et al., 2013, Continuous exhumation of mantle-derived rocks at the Southwest Indian Ridge for 11 million years: *Nature Geoscience*, v. 6, p. 314–320, <https://doi.org/10.1038/ngeo1771>.

Searle, R.C., MacLeod, C.J., Peirce, C., and Reston, T.J., 2019, The Mid-Atlantic Ridge near 13°20'N: High-resolution magnetic and bathymetry imaging: *Geochemistry Geophysics Geosystems*, v. 20, p. 295–313, <https://doi.org/10.1029/2018GC007940>.

Simão, N.M., Peirce, C., Funnell, M.J., Robinson, A.H., Searle, R.C., MacLeod, C.J., and Reston, T.J., 2020, 3-D *P*-wave velocity structure of oceanic core complexes at 13°N on the Mid-Atlantic Ridge: *Geophysical Journal International*, v. 221, p. 1555–1579, <https://doi.org/10.1093/gji/ggaa093>.

Smith, D.K., Escartín, J., Schouten, H., and Cann, J.R., 2008, Fault rotation and core complex formation: Significant processes in seafloor formation at slow-spreading mid-ocean ridges (Mid-Atlantic Ridge, 13°–15°N): *Geochemistry Geophysics Geosystems*, v. 9, Q03003, <https://doi.org/10.1029/2007GC001699>.

Yu, Z.T., Li, J.B., Niu, X.W., Rawlinson, N., Ruan, A.G., Wang, W., Hu, H., Wei, X.D., Zhang, J., and Liang, Y.Y., 2018, Lithospheric structure and tectonic processes constrained by micro-earthquake activity at the central ultraslow-spreading Southwest Indian Ridge (49.2° to 50.8° E): *Journal of Geophysical Research: Solid Earth*, v. 123, p. 6247–6262, <https://doi.org/10.1029/2017JB015367>.

Printed in USA